

Investigations of heterogeneous diffusion based on the probability density of scaled squared displacements observed from single molecules in ultra-thin liquid films

*Michael Bauer, Mario Heidernätsch, Daniela Täuber,
Christian von Borczyskowski, Günter Radons*

Chemnitz University of Technology, Institute of Physics, Germany

Corresponding author:

Michael Bauer
Institute of Physics
Chemnitz University of Technology
Reichenhainer Straße 70
09126 Chemnitz, Germany
E-Mail: michael.bauer@physik.tu-chemnitz.de

Abstract

Diffusion processes in ultra-thin liquid films observed by video microscopy reveal a complex behavior. In contrast to homogeneous diffusion, dynamic and static heterogeneities are induced by layer transitions and compartments with differing diffusion coefficients, respectively. The objective of this research is the detection and distinction of such heterogeneities as well as an analysis of the underlying processes. Hence, a new method is proposed establishing a probability density of scaled squared displacements. This probability density allows for a simple and well-defined calculation of time-dependent diffusion coefficients and its fluctuations. Furthermore, by simulating a heterogeneous diffusion process these results are verified and compared to mean square displacement calculations. By means of the simulated probability density data, their dependency on the parameters is illustrated and further implications are pointed out.

keywords: diffusion, dynamic and static heterogeneity, scaled squared displacements

1. Introduction

Investigating diffusing molecules in liquid films by video microscopy offers an interesting field of research. Within the liquid film the fluorescent molecules conduct a three-dimensional diffusion process caused by collisions with the particles of the liquid. However, the three-dimensional trajectory is observed by video microscopy. The resulting video of the diffusing molecules corresponds to the two-dimensional projection of the actual movement. Thus, the projected trajectory lacks information about the third dimension. As a consequence, a change in the third dimension and therefore in the diffusion properties of the molecules cannot be observed directly. Nevertheless, it influences the molecule's projected trajectory and might be detected by improved analysis.

In an experimental setup, the projected position of a tracked particle can be measured directly. A recently developed tracking method [1] determines the positions of the molecules accurately even if blinking effects of the fluorescent molecule interrupts its visible trajectory. The position of the particle is extracted at two times characterized by a time difference τ . It results from the observation time or the measurement process. Thus in video microscopy, the lower limit is given by $\tau_{\min} \leq \tau$, which is related to the inverse of the frame rate. It represents the smallest resolvable variation in time for observing the particles' movements. From the difference of the two positions the corresponding squared displacement is obtained by calculating

$$(\Delta \mathbf{r}(\tau))^2 := (\mathbf{r}(t+\tau) - \mathbf{r}(t))^2. \quad (1)$$

Due to their close relation to diffusion coefficients squared displacements are often used for data analysis. In particular, squared displacements are averaged over time t or over all particles to obtain a mean square displacement graph $\langle (\Delta \mathbf{r}(\tau))^2 \rangle$ versus τ . Then, the slope of the mean square displacement is related to the diffusion coefficient according to the Einstein-Smoluchowski-equation [2]. As a result, the mean diffusion coefficient of the observed molecule can be determined.

In general, the method of mean square displacement calculations yields sufficient information for homogeneous isotropic diffusion, where only one diffusion constant exists. However, diffusing molecules in ultra-thin liquid films reveal a more complex behavior [3]. A convincing picture is given in [4] describing a layering of liquids at solid interfaces leading to inhomogeneous diffusion. As a consequence, a layer model for such systems was developed. It involves a layer-dependent diffusion coefficient. Further, the molecules have the ability to switch between the layers during their diffusion process. In a projection as performed in experiments, the jumping between layers appears as a dynamical, random switching between different diffusion coefficients. This process results in so-called dynamic heterogeneities. Moreover, recent experimental observations indicate the existence of impurities on the substrate. They result in an altered diffusion coefficient in such a region due to gliding via silanol bridging [5] or a slowdown of diffusion [6,7]. Thus, the diffusion process is additionally influenced by static heterogeneities. A correct analysis of the observed inhomogeneous diffusion process constitutes the necessity to detect static and dynamic heterogeneities. Thus, besides mean square displacement calculations new methods have to be established in order to distinguish between both inhomogeneities and extract their parameters. The drawback of determining mean square displacements lies in the information loss caused by the averaging procedure. It conceals the effects caused by the existence of several different diffusion coefficients.

To investigate the behavior of such an inhomogeneous system with N layers, a simulation of the diffusion process is carried out. The model is defined by

$$\frac{\partial}{\partial t} p_n(\mathbf{r}, t) = \sum_m [w_{nm} p_m(\mathbf{r}, t) - w_{mn} p_n(\mathbf{r}, t)] + D_n \nabla^2 p_n(\mathbf{r}, t) \quad \text{with } m, n \in \{1, \dots, N\} \quad (2)$$

a system of N partial differential equations for the probability densities $p_n(\mathbf{r}, t)$ for finding the particle at time t at position $\mathbf{r} = (x, y)$ in the n -th layer. In Eq. 2, w_{nm} denotes the transition rate from layer m to layer n , and D_n is the diffusion constant in the n -th layer. The mean dwell time \hat{t}_m in layer m is determined by the transition rates via

$$\hat{t}_m = \left(\sum_n w_{nm} \right)^{-1}. \quad (3)$$

Hence, the movement of a diffusing molecule is modeled by ordinary two-dimensional diffusion within a layer interrupted by jumps between layers governed by a master equation. Since in experiment two-dimensional projections of this process are observed, the statistics of these observations are governed by the projected probability density

$$p(\mathbf{r}, t) = \sum_n p_n(\mathbf{r}, t). \quad (4)$$

This projection of the diffusion process onto the two-dimensional plane and the jump process between layers with distinct diffusion coefficients induce the dynamic heterogeneity. Furthermore, the static heterogeneity is modeled by a compartment with a different diffusion coefficient in the base layer next to the substrate. If a molecule enters this particular region it diffuses with the given diffusion coefficient deviating from the ordinary coefficient in the base layer.

For a system comprising only two layers further analytical results can be deduced. By integrating Eq. 2 over all positions \mathbf{r} within a layer, as a result the master equation

$$\frac{d}{dt} p_n(t) = \sum_m [w_{nm} p_m(t) - w_{mn} p_n(t)] \quad \text{with } m, n \in \{1, 2\} \quad (5)$$

is obtained describing a two-state Markov process. The equilibrium layer probabilities π_1 and π_2 are easily obtained from detailed balance as

$$\pi_1 = \frac{w_{12}}{w_{12} + w_{21}} \quad \text{and} \quad \pi_2 = \frac{w_{21}}{w_{12} + w_{21}}. \quad (6)$$

With this equilibrium distribution, the mean diffusion coefficient of the bi-layer system as obtained e.g. from a long-term measurement of the mean square-displacement, can be calculated as

$$\bar{D} = D_1 \pi_1 + D_2 \pi_2 \quad (7)$$

a weighted sum of the diffusion coefficients of the two layers.

In conclusion, the three-dimensional diffusion process is modeled by a two-dimensional random walk and an additional jump process. Due to the projection and embedded compartments, the simulated data contain both dynamic and static

heterogeneities. Therefore, it resembles the inhomogeneous diffusion process observed experimentally. Consequently, improved investigation methods and related findings tested with the simulated data can be applied to real experimental data.

A model of a bi-layer system with thickness 2-10 nm is illustrated in Fig. 1. The dynamic heterogeneity originates from the layers with their distinct diffusion coefficients. Furthermore, the base layer next to the substrate comprises a compartment with a third diffusion coefficient. Hence, a model with both static and dynamic heterogeneities is established.

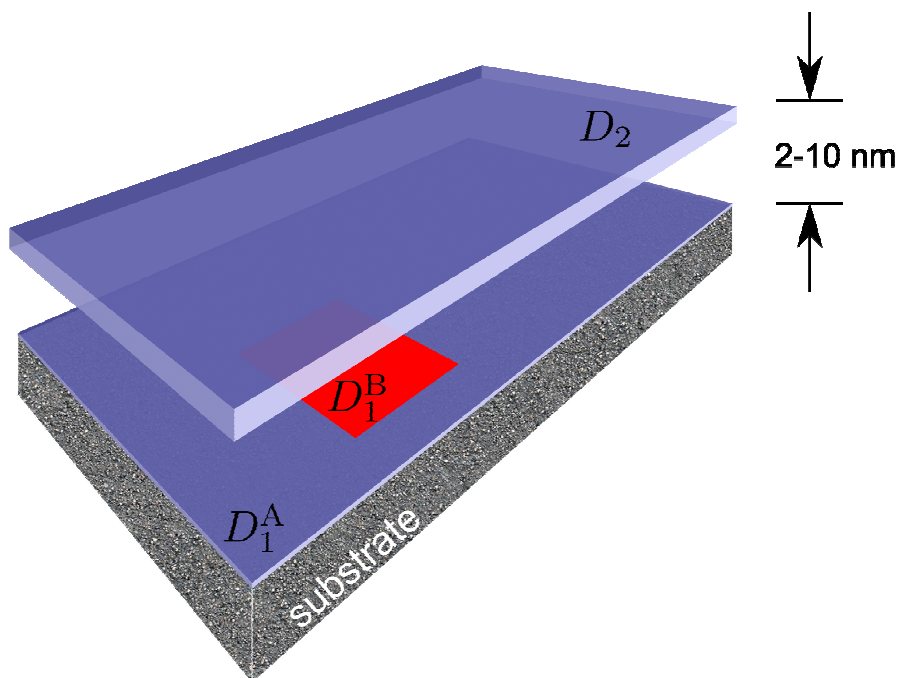


Fig. 1: The bi-layer system is used for the simulation of a molecule's trajectory. Dynamic heterogeneity is induced by the two layers with their distinct diffusion coefficients. Within the red-colored compartment in the base layer next to the substrate the diffusion can be modified providing a static heterogeneity.

It is the objective of this research to develop advanced methods for the analysis of such inhomogeneous diffusion processes. This is necessary since investigations based on homogeneous diffusion are no longer appropriate if heterogeneities are involved. However, investigations in this article are restricted to dynamic heterogeneities since static heterogeneities will be covered in future work. Furthermore, a connection to the commonly used analysis via mean square displacements is established. To validate the theoretical considerations, the proposed methods have been applied to the diffusion of

Rhodamine B dye molecules in ultra-thin liquid films of TEHOS and have been compared to previous results [8].

2. Probability density of scaled squared displacements

The measurement of squared displacements represents a common approach to analyze the properties of a diffusion process. However, these squared displacements are directly related to the time difference τ for which they are measured. Since the variance of the particles' positions of a Wiener process grows with increasing time interval, the particles can explore a larger area. Exactly this is achieved by increasing the time between two observations of the particle. Hence, the squared displacements depend on τ and will be larger for longer measurement time intervals or lower frame rates. To remove this trivial time dependency, the squared displacements are divided by the given time interval τ . The resulting expression $(\Delta\mathbf{r}(\tau))^2 / \tau$ has the dimension of a diffusion coefficient, but it is a fluctuating quantity e.g. along a trajectory. Even after averaging, it is in general still dependent on τ . This could be understood by considering an inhomogeneous diffusion process since the size of the squared displacements is subject to the diffusion coefficient as well. Depending on the dwell times in the layers and their relation to the measurement time, transitions between the layers might be conducted. Thus, during the diffusion between two measured positions several distinct diffusion coefficients affect the displacement. This effect will be reduced if the measurement time is very small compared to the dwell time in the current layer. Even though, the displacements observed in an inhomogeneous diffusion process are still governed by different diffusion coefficients.

The properties of a diffusion process are analyzed from the observed displacements by a new method. For that reason, a probability density $p(D, \tau)$ is established by the distribution of the scaled squared displacements. Formally, it is given by

$$p(D, \tau) = \left\langle \delta \left(D - \frac{(\Delta\mathbf{r}(\tau))^2}{2d \tau} \right) \right\rangle, \quad (8)$$

where $\langle \dots \rangle$ denotes a time or an ensemble average, both coinciding if the system is ergodic. Naturally, the probability density is normalized since

$$\int_0^{\infty} p(D, \tau) dD = 1 \quad (9)$$

is fulfilled for any $p(D, \tau)$. Furthermore, the probability densities can be used to calculate mean values and variances as well as higher moments and cumulants of their distribution. Experimental data approximate such a probability density by binning the samples in a normalized histogram. This can be generated from the experimental samples with little effort.

The probability density of the scaled squared displacements offers several features. In general, it is dependent on the observation time τ since the squared displacements

comprise this dependency. By determining the first moment of the probability density, an ordinary diffusion coefficient

$$\bar{D}(\tau) = \int_0^{\infty} D p(D, \tau) dD = \frac{\langle (\Delta \mathbf{r}(\tau))^2 \rangle}{2d \tau} \quad (10)$$

is obtained. In the limit $\tau \rightarrow 0$, $\bar{D}(\tau)$ equals the diffusion coefficient appearing e.g. in the Fokker-Planck equation [9]. In the opposite limit $\tau \rightarrow \infty$, $\bar{D}(\tau)$ is equal to the long-term increase of the squared displacements appearing e.g. as the slope of the mean square displacement [2]. Thus, a connection between a microscopic diffusion coefficient in the Fokker-Planck equation and a macroscopic diffusion coefficient in mean square displacement calculations is established.

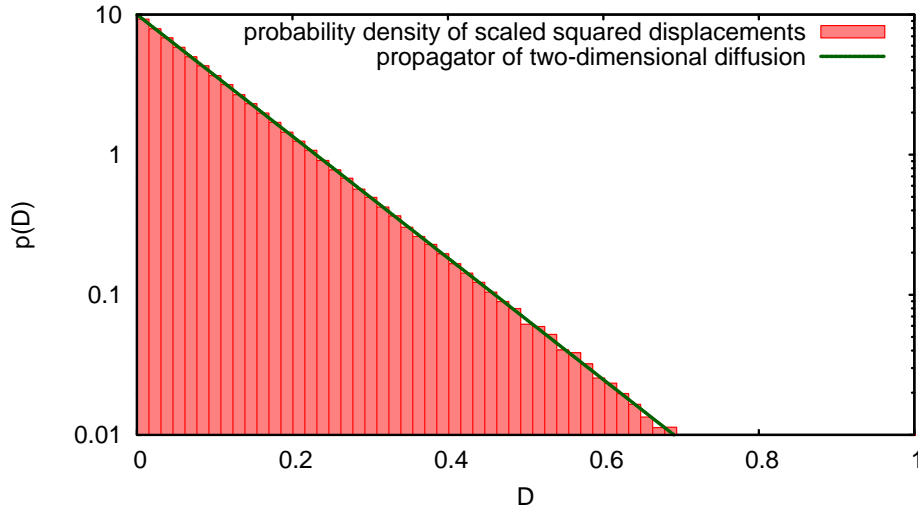


Fig. 2: The probability density of scaled squared displacements exhibits a mono-exponential behavior in case of a homogeneous, two-dimensional diffusion process. The propagator is accordance with the histogram.

In the special case of homogeneous diffusion processes the τ dependency in Eq. 10 vanishes. Then, $\bar{D}(\tau) = D_0$ becomes independent of τ , and D_0 denotes the diffusion coefficient of the system. In accordance with this also $p(D, \tau) = p(D)$ becomes τ -independent and can be expressed analytically. Dependent on the dimensionality d of the system, it can be easily calculated as

$$p(D) = \frac{1}{\sqrt{2\pi D_0}} \frac{1}{\sqrt{D}} \exp\left(-\frac{D}{2D_0}\right) \quad \text{for } d=1 \quad (11)$$

$$p(D) = \frac{1}{D_0} \exp\left(-\frac{D}{D_0}\right) \quad \text{for } d = 2 \quad (12)$$

and

$$p(D) = \frac{1}{\sqrt{2\pi}} \left(\frac{3}{D_0}\right)^{\frac{3}{2}} \sqrt{D} \exp\left(-\frac{3}{2} \frac{D}{D_0}\right) \quad \text{for } d = 3 \quad (13)$$

It is obvious, that the normalization Eq. 9 holds in all cases.

For the investigated model of a bi-layer system, Eq. 12 for $d = 2$ is of special interest. Hence, the probability density features an exponential decay parameterized by the underlying diffusion coefficient. This behavior can be identified as a straight line in a log-linear plot. As an illustration, this is shown in Fig. 2 depicting a probability density of a homogeneous diffusion process. Therein, the mono-exponential behavior can clearly be identified.

For a diffusion process involving dynamic heterogeneities the probability density exhibits a more complicated, non-exponential structure. The reason is the interference of distinct propagators caused by jumps. If the molecule changes its layer during the measurement time τ , the diffusion will take place with a mean diffusion coefficient corresponding to the involved layers. This mean originates from the weighting of the diffusion coefficients with the total dwell time in each layer with respect to the measurement time. Consequently, propagators which belong to intermediate diffusion coefficients are introduced contributing to the probability density. For this model it can be shown analytically that the probability density is not the superposition of two exponentials originating from the propagators of the diffusion coefficients in the layers. Thus, a multi-exponential fit according to the number of included layers does not yield appropriate results. Likewise static heterogeneities lead to a similar effect.

Furthermore, the probability density of scaled squared displacements can be transformed into an integrated density

$$P(D, \tau) = \int_D^\infty p(D', \tau) dD', \quad (14)$$

which offers other advantages. Conversely, the probability density $p(D, \tau)$ is the differentiated expression of a cumulative scaled squared step size distribution. Similarly, [10] analyzed ranked unscaled squared step size distributions. In [10] bi-exponential fits are used in order to estimate the diffusion coefficients. This seems to offer an easy approach to determine the parameters of the underlying system. However, since the probability density is strongly dependent on the measurement time τ in comparison to the dwell times, only for small τ appropriate results are obtained. For larger τ , resulting fit parameters can deviate significantly from the actual diffusion coefficients. Furthermore, the probability density of scaled squared displacements can also be used to analyze diffusion in channels as investigated in [11]. Due to the confinement of the particles the probability density may be described more appropriately by functional dependencies as in

Eq. 11 corresponding to one-dimensional diffusion processes. However, the dependency on the measurement time may not be neglected since it can lead to inappropriate results.

3. Simulation of heterogeneous diffusion

For the analysis of the diffusion process via scaled squared displacements artificial data are created by simulations. Therefore, a system consisting of two layers with diffusion coefficient $D_1 = 0.1 \text{ m}^2 \text{ s}^{-1}$ in the base layer and $D_2 = 1.0 \text{ m}^2 \text{ s}^{-1}$ in the second layer is used. This system contains only dynamic heterogeneities since no compartment is incorporated. The jump rates between the layers are varied leading to a change in the dwell times as well. Despite that, the equilibrium distribution between the layers remained constant as $\pi_1 = \frac{1}{3}$ and $\pi_2 = \frac{2}{3}$, respectively. According to Eq. 7, the given parameters yield a mean diffusion coefficient $\bar{D} = 0.7 \text{ m}^2 \text{ s}^{-1}$ exactly. This value is used to verify the results from mean square displacement calculation as well as via the probability density $p(D, \tau)$.

The diffusion simulation is accomplished with 1000 time steps of time interval 0.01 s generating a trajectory of total length 10 s. Moreover, 1000 such trajectories are created simultaneously. It should be noted, that the distribution of the random walkers between the two layers is initialized with the corresponding stationary distribution. Thus, a transient behavior is omitted, because the walkers do not have to distribute among the layers. The analysis investigates the dynamical behavior of an equilibrated system.

For the determination of the scaled squared displacements different measurement times are investigated, where $\tau = 0.05$ s is chosen as the smallest one. It resembles a frame rate of 20 frames per second in video microscopy. Due to the discrete time step of the simulation up to five jumps are allowed within this measurement time. Indeed depending on the jump rates between the layers this is more or less likely.

During the simulation all occurring squared displacements are gathered. They are scaled by the corresponding measurement time τ and divided by a dimensionality factor of 4 due to the two-dimensional diffusion process. In total, 1 million scaled squared displacements are captured. They are grouped in a histogram consisting of 100 equally spaced bins. After the simulation has finished, the histogram gets normalized to obtain a probability density.

4. Investigation of simulated data

In a first simulation, the dependency of the probability density of scaled squared displacements on the measurement time τ is investigated. For this purpose, measurement time and transition rates are chosen to emphasize the properties of this dependency. In particular, the transition rate from the base layer to the second layer equals $w_{21} = 8.0$ jumps per second. In other words, on average this transition takes place after $\hat{t}_1 = 0.125$ s of diffusion in the base layer. The backward jump rate into the base layer is given by $w_{12} = 4.0$ jumps per second. Thus, the mean dwell time in the second layer is equal to $\hat{t}_2 = 0.25$ s. According to Eq. 6, the proportion of the jump rates to their sum

results in the equilibrium distribution between the layers and satisfies the specified π_1 and π_2 . Based on the same simulation data, the squared displacements are gathered using different measurement times τ . Starting with $\tau=0.05$ s, almost no layer transition is accomplished between the observed positions. Thus, the diffusion processes in each layer are separated quite properly. However, by increasing τ to 0.2 s it gets into the critical range of the dwell times. As a consequence, the diffusion between two observed positions can have changed its coefficient several times. This effect is even more amplified for larger τ . Due to several layer transitions only a mean diffusion coefficient is observed.

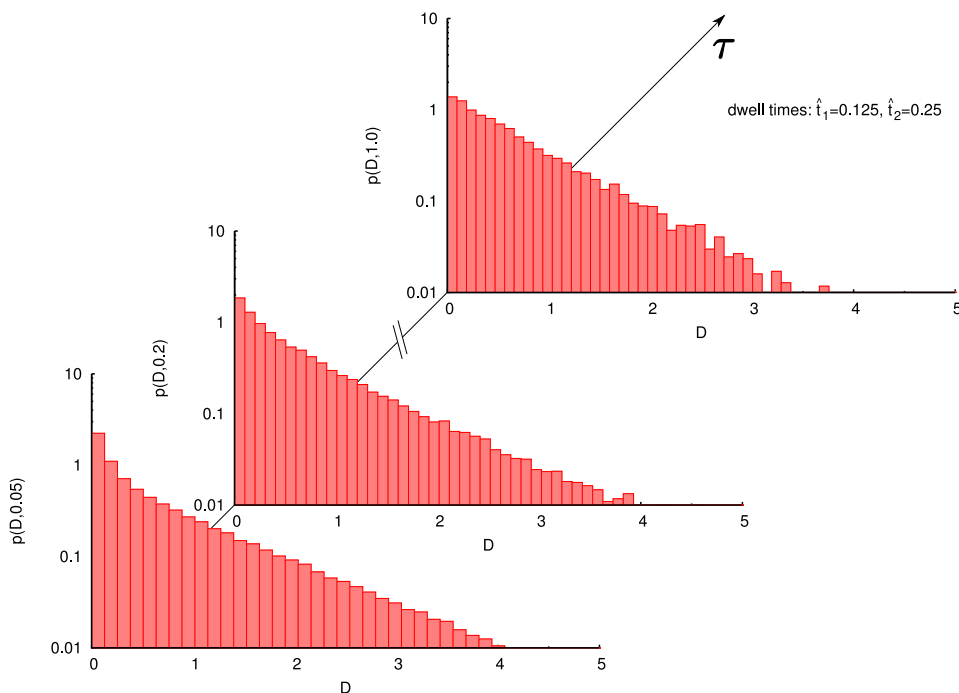


Fig. 3: The probability density of scaled squared displacements reveals a non-trivial dependency on the measurement time τ . The non-exponential decay converges to an exponential behavior in the limit τ to infinity. Hence, only for small τ heterogeneous diffusion is distinguishable from homogeneous one.

The probability densities belonging to $\tau=0.05$ s, $\tau=0.2$ s and $\tau=1.0$ s are depicted in Fig. 3. Despite the scaling of the squared displacements to remove their trivial time dependency their densities are still influenced by τ . By means of the fluctuations in the probability density of the scaled squared displacements, heterogeneities in an investigated system can be detected easily. Those fluctuations, e.g. the variance of the probability density, can be quantified through the calculation of higher moments analogous to Eq. 10. By averaging over those fluctuations e.g. in mean square displacement calculations,

information about heterogeneities is eliminated. It can be derived analytically, that for $\tau \rightarrow \infty$ the probability density exhibits a convergence to a mono-exponential decay parameterized by the mean diffusion coefficient \bar{D} of the system as given by Eq. 7. In Fig. 3 it is obvious that the non-exponential decay converges to a mono-exponential behavior for increasing τ . Simultaneously, the values of the density are adapted since the histogram still has to be normalized to 1 according to Eq. 9. As discussed previously, the probability densities are dependent on τ in a non-trivial way. The reasons are the intermediate propagators, which govern the diffusion of the molecules during observation. In the limit of infinite τ , the probability density resembles that of a homogeneous diffusion process complicating a distinction. However, for small τ the probability density of scaled squared displacements of an inhomogeneous diffusion process can be distinguished from that of a homogeneous one without difficulty.

In a second step, the first moments of the probability densities are verified to be equivalent to the mean diffusion coefficient \bar{D} . This is confirmed by multiplying each histogram bin's area, which is equal to the probability, with its corresponding scaled squared displacement. Finally, it is summed over all these products. For the three different τ mean diffusion coefficients of $0.705 \text{ m}^2\text{s}^{-1}$, $0.698 \text{ m}^2\text{s}^{-1}$ and $0.699 \text{ m}^2\text{s}^{-1}$ are obtained respectively. As expected, the values are independent of τ and in good agreement with the analytically predicted value.

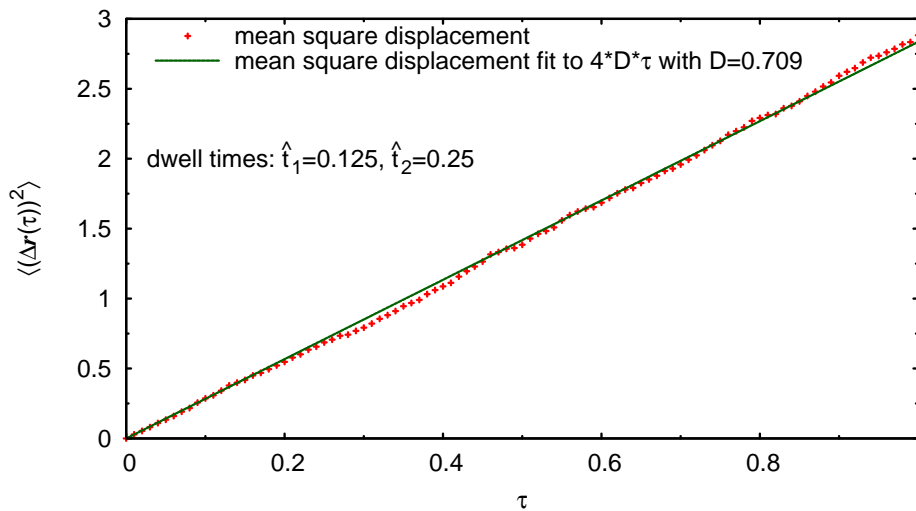


Fig. 4: The commonly used mean square displacement versus measurement time τ can be fitted with a linear function. The fit parameter yields the mean diffusion coefficient. Due to the involved averaging, the heterogeneities of the system are obscured in contrast to Fig. 3.

Moreover, for the same transition rates the mean square displacement $\langle(\Delta\mathbf{r}(\tau))^2\rangle$ versus τ is depicted in Fig. 4. The uniform slope is a consequence of the initial equilibrium distribution between the layers omitting any transient behavior. Thus, the dependency of the mean square displacement on the measurement time τ does not reveal any heterogeneity of the system. In contrast, the probability density of the scaled squared displacements clearly exposes this dependency as presented in Fig. 3. This allows the detection of an inhomogeneous diffusion process.

To validate the mean diffusion coefficient, a fit of the mean square displacement is calculated as illustrated in Fig. 4. The fitted value of $0.709\text{ m}^2\text{s}^{-1}$ deviates only slightly from the analytical value. Thus, the method of determining the first moment of the probability density yields the same value as by mean square displacement calculation. However, to obtain an accurate value for the fit, large τ are necessary requiring sufficiently long trajectories [2]. In contrast, for the probability density of scaled squared displacements only short segments of trajectories are sufficient, and the mean diffusion coefficient can be calculated precisely.

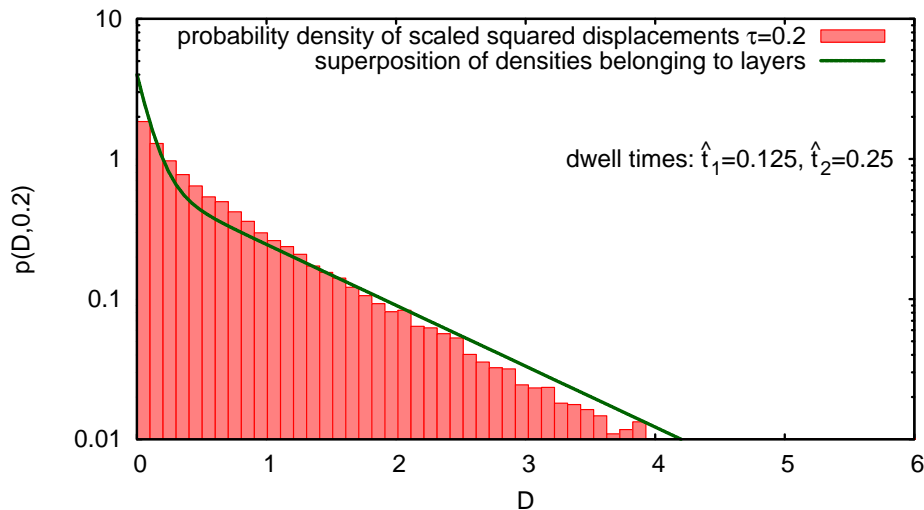


Fig. 5: The probability density of the observed scaled squared displacements for measurement time $\tau=0.2\text{ s}$ does still not show a mono-exponential behavior. Due to the dwell times of the layers being in the same range as τ , the probability density cannot be approximated by a superposition of the two densities belonging to the layers. The deviations increase with larger τ , and thus a bi-exponential fit will lead to inappropriate results.

In general, the propagator of the bi-layer system is not the superposition of the two propagators belonging to the diffusion processes in the layers. This becomes obvious especially in the limit of infinite τ , where the probability density reveals a mono-

exponential behavior. This cannot be accomplished by a weighted superposition of two different mono-exponentially decaying densities. To illustrate this, the existing deviation is depicted in Fig. 5. For a measurement time $\tau=0.2$ s, which is approximately in the range of the dwell times, the histogram and the superposition of the densities modelling two separate diffusion processes differ significantly. Hence, the propagator of the full system cannot be expressed by superimposing the two propagators of the diffusion processes in the layers. The reason lies in the change of the diffusion coefficient caused by layer transitions. As a consequence, a bi-exponential fit could not generate appropriate results for the involved diffusion coefficients and has to be avoided. This has to be considered for experimental data, since the dwell times in the layers are often unavailable preventing an accurate estimation of fitted diffusion coefficients.

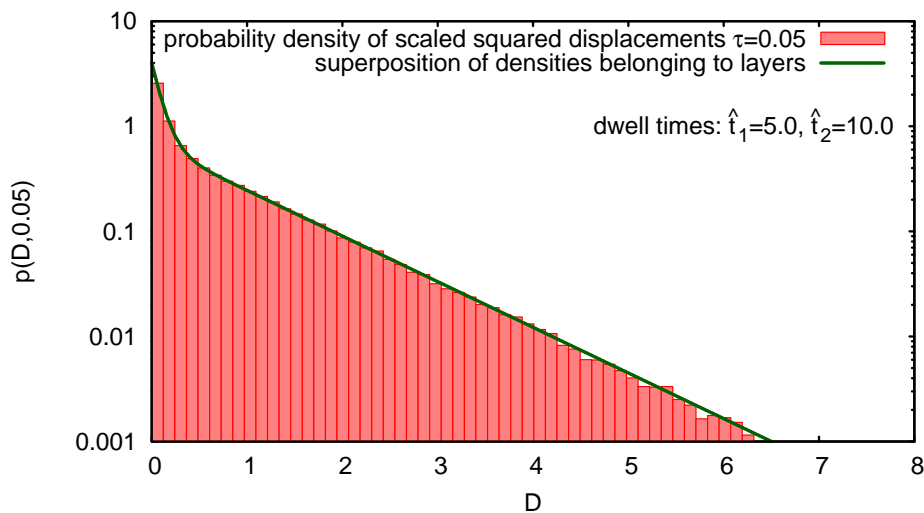


Fig. 6: The probability density of the observed scaled squared displacements from a diffusion process with dynamic heterogeneity deviates from a mono-exponential decay. Due to small measurement time τ compared to the dwell times, the density can be approximated appropriately by the superposition of the densities which belong to the two diffusion coefficients of the system.

In another simulation the transition rates of the bi-layer system are decreased. They are defined in a way to suppress fast oscillating layer transitions. In particular, jump rates of $w_{21} = 0.2$ and $w_{12} = 0.1$ jumps per second result in mean dwell times in each layer of $\hat{t}_1 = 5$ s and $\hat{t}_2 = 10$ s, respectively. Due to the long dwell times compared to the short measurement time $\tau=0.05$ s, the predominant part of the observed squared displacements does not include any layer transition. The observation detects apparently separated diffusion processes in each layer as though their interference vanishes. Therefore, the probability density can be described by a superposition of the propagators corresponding

to the two diffusion coefficients in a good approximation. The weights of the propagators are defined by the equilibrium distribution between the associated layers as given in Eq. 6.

The probability density of the observed scaled squared displacements is depicted in Fig. 6. The effect of the dynamic heterogeneity becomes apparent since the probability density deviates from the mono-exponential decay obtained by homogeneous diffusion as shown in Fig. 2. Furthermore, for short measurement times τ compared to the dwell times in the layers, the diffusion processes can be separated. Caused by the long dwell times in each layer, the density of the heterogeneous system is reasonably well approximated by the superposition of the densities belonging to two separate diffusion processes. The accordance of the superimposed densities with the normalized histogram is illustrated in Fig. 6. Consequently, this enables an estimation of the diffusion coefficients via a bi-exponential fit, which is quite common in the diffusion community.

5. Conclusion

A new method was presented in order to analyze diffusing molecules from video microscopy. It is based on scaled squared displacements and their probability density. This offers an advantage for experimental data since short trajectories are sufficient. Based on numerical simulations the proposed method could be verified. Featuring an efficient calculation, it reproduced mean diffusion coefficients as obtained by the mean square displacement. Furthermore, the probability density of scaled squared displacements contains more information of the observed diffusion process than mean square displacement data since the full distribution and not only its first moment is involved. This becomes apparent in the non-trivial time dependency of the probability density of scaled squared displacements. Thus, the microscopic investigation of the diffusion process enables the detection of heterogeneities. In future research, further features existing in this probability density have to be explored. Especially, an auto-convolution of the probability density promises refined possibilities to detect the involved diffusion coefficients.

A region-dependent capturing of scaled squared displacements offers access to diffusion processes influenced by compartments. Thus, generating a map of probability densities of scaled squared displacements seems to be an encouraging approach to detect and analyze both dynamic and static heterogeneities.

Acknowledgements

We acknowledge financial support by the German Research Foundation (DFG) for funding of the research unit FOR 877 “From Local Constraints to Macroscopic Transport”.

References

- [1] M. Heidernätsch, M. Bauer, D. Täuber, G. Radons, C. von Borczyskowski, *Diffusion Fundamentals*, 2009.
- [2] H. Qian, M.P. Sheetz, E.L. Elson, *Biophys. J.* 60(4):910-921, 1991.
- [3] J. Schuster, F. Cichos, C. von Borczyskowski, *Eur. Polymer J.* 40(5):993-999, 2004.
- [4] C.-J. Yu et al., *Phys. Rev. Lett.* 82(11):2326-2329, 1999.
- [5] A. Honciuc, A.W. Harant, D.K. Schwartz, *Langmuir* 24(13):6562-6566, 2008.
- [6] J. Schuster, F. Cichos, C. von Borczyskowski, *Eur. Phys. J. E* 12 019, 2003.
- [7] I. Trenkmann, J. Schuster, S. Gangopadhyay, C. von Borczyskowski, *Diffusion Fundamentals*, 2009.
- [8] D. Täuber, M. Heidernätsch, M. Bauer, G. Radons, J. Schuster, C. von Borczyskowski, *Diffusion Fundamentals*, 2009.
- [9] H. Risken, *The Fokker-Planck equation: methods of solution and applications*, Springer, Berlin, second edition, 1996.
- [10] C. Hellriegel, J. Kirstein, C. Bräuchle, V. Latour, T. Pigot, R. Olivier, S. Lacombe, R. Brown, V. Guieu, T. Payaraste, A. Izquierdo, P. Mocho, *J. Phys. Chem. B* 108, 14699-14709, 2004.
- [11] J. Kirstein, B. Platschek, C. Jung, R. Brown, T. Bein, C. Bräuchle, *Nature Materials* 6, 303-310, 2007.